Calorimetric Measurements of Thermal Control Surfaces at Geosychronous Orbit

C. C. Anderson* and M. M. Hattar†
Aerojet ElectroSystems Company, Azusa, California

Calorimeter data for up to 18,000 equivalent sun-hours are presented for a number of satellite thermal control surfaces. This has been an ongoing study by Aerojet ElectroSystems. Solar absorptance values as a function of time were collected at geosynchronous orbit on samples of zinc orthotitanate paint, silver-alumina-silica, silvered Teflon, aluminized Teflon, silica cloth, and clean second-surface mirrors. Over 6000 equivalent sun-hours of calorimeter data were also collected on precontaminated second-surface mirror samples (also on-orbit). A useful collection of solar absorptance degradation equations is the result. These equations are of major significance in predicting satellite useful life.

Nomenclature

t	=	time
T	=	temperature
a_m	=	maximum solar absorptance
a_o	=	initial solar absorptance
a_s	=	solar absorptance
ξ	=	emissivity
τ	=	time constant

Introduction

An important aspect of satellite thermal management is the careful selection of thermal control surface coatings. The general warming trends that are seen on satellites can be minimized by using thermal control surface coatings that have stable thermal/optical characteristics. For more than seven years on-orbit, calorimeter data, initially presented in Refs. 1 and 2, have been obtained for samples of thermal control surface treatments from six different operational satellites in geosynchronous orbit. Presented are solar absorptance (a_s) values that were derived as a function of equivalent sun-hours (ESH) for samples of zinc orthotitanate (ZOT) paint, silver-aluminia-silica (SAS), silvered Teflon, aluminized Teflon, silica cloth, and clean second-surface quartz mirrors. Also presented are calorimeter data for 6000 equivalent sun-hours of a_s data on samples of second-surface fused silica mirrors coated with two different thicknesses of polydimethylphenyl siloxane (PDPS). The PDPS coating was intended to simulate contaminants from silicon-based products used on spacecraft that are expected to outgas in the space environment. These a_s data are compared to other relevant data from the literature and to additional a_s degradation measurements made on other surfaces of these satellites. Applications of these comparison data are also discussed.

Contaminant build-up on a surface and subsequent photolysis and/or polymerization of the contaminant is one mechanism that increases a_s. Contaminants can be the result of out-gassing of volatile condensible materials from materials used on spacecraft. It is critical that materials with low out-gassing characteristics be used if low a_s degradation rates are to be achieved. Contamination can also result from satellite and spacecraft handling on the ground. The launch environment and subsequent booster firings can also cause contamination. Breakdown of the thermal control surface from exposure to ultraviolet radiation, protons, and electrons can also cause an increase in a_s. Also, deterioration of satellite and spacecraft materials caused by the cyclic thermal-vacuum environment could contribute to increased degradation rates.

Received April 23, 1987; presented as Paper 87-1571 at the AIAA 22nd Thermophysics Conference, Honolulu, HI, June 9, 1987; revision received Sept. 3, 1987. Copyright © American Institute of Aeronautics and Astronautics, Inc., 1987. All rights reserved.

*Project Engineer, Space Surveillance Division.
†Member Technical Staff, Space Surveillance Division.

Calorimeter Design

The same calorimeter design is used on all six flights.[1] The calorimeter is located in the same position on each satellite. A cross-section of the calorimeter is shown in Fig. 1. The design intent is to thermally isolate the samples of thermal control surfaces for ease and reliability of analysis. This is accomplished by using thin-walled fiberglass supports that were vacuum-deposited with aluminum to minimize radiation heat transfer within the calorimeter. Multi-layer insulation is used to decouple the samples from the calorimeter housing. In addition, strips of silvered Teflon are used to close the gaps between samples to prevent solar energy from reaching the housing enclosure. A thermal sensor was placed beneath each sample. An additional thermal sensor was mounted on the inside of the housing baseplate to help determine the heat leak of the samples. The location of the calorimeter was chosen because of the very small view factor (less than two percent) to the external surfaces of the spacecraft. This location on the

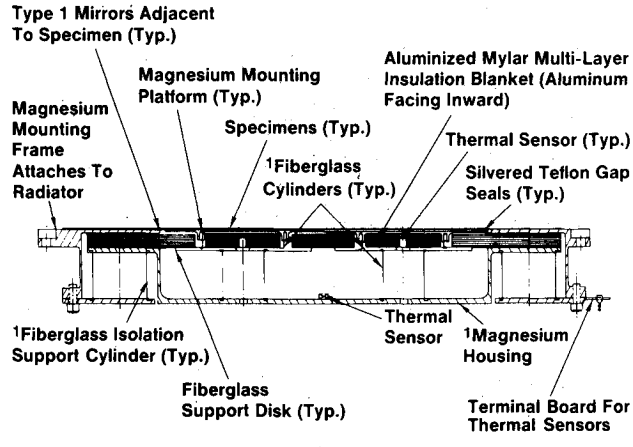

Fig. 1 Cutaway view of calorimeter design.

satellite is also less susceptible to contamination from other spacecraft components. This design was flown successfully on all six flights.

Calorimeter Data Analysis Method

A SINDA computer model was developed to analyze the calorimeter data.[2] The model consists of 23 nodes of which several are boundary nodes, external surfaces of the satellite that have a view of the calorimeter. The seasonal effects of solar heat flux and orbit inclination are included in the model.

The algorithm interates a_s values until the maximum temperature of the samples matches the SINDA model maximum temperatures. A flow chart of this algorithm is found in Ref. 1. The estimated error in the absolute solar absorption is $+.009, -.006$.[1]

This analysis assumes that the emissivity, ξ, remains constant. This has been substantiated by earlier reports[1,2] and with data from recent samples flown on Satellite 1.

The analysis of calorimeter data for each satellite was performed at approximately two-month intervals.

Thermal Control Surface Samples

Descriptions

Table 1 describes in detail all thermal control surface samples and the method of application for each. These samples were chosen for their low a_s/ξ characteristics, weight, and space-stability. These samples include metalized Teflon, silica cloth, ZOT paint, and SAS. References 1 and 2 describe the samples on Satellites E through H. A detailed description of the samples on Satellite I follows.

The four thermal control surface samples on the recently flown Satellite I are a second-surface mirror (SAS) and two second-surface mirrors coated with different thicknesses of PDPS. The second-surface mirror is a contaminant-free, silver-backed quartz mirror included in the calorimeter as a reference. The SAS is a low-absorptance, multilayered interference coating that is vacuum-deposited on a specular aluminum substrate. The substrate for the SAS is reflector grade 1100 aluminum. A coating of 400 Å of inconel is deposited on the aluminum to provide a diffusion barrier to the silver layer; 800 Å of silver is deposited on the inconel; 3300 Å of aluminum oxide is deposited on the silver; and 850 Å of silicone oxide is deposited on the aluminum oxide. The SAS samples were prepared using the information provided in Refs. 3-5. A detailed description of the PDPS samples is given in Ref. 10.

Results

Calorimeter data are converted from days-after-launch to equivalent sun-hours so that these resulting data may be used in various design applications. Equivalent sun-hours is the number of hours of one full sun exposure. One year after launch is equivalent to 2400 sun-hours for these calorimeter samples, based on their location and view factor to the sun. Figure 2 updates representative calorimeter data presented in Ref. 1 for Satellites D, E, F, G, and H. Data for Satellites A and B are given in Ref. 2. No data are available from Satellite C. The a_s for the four samples on Satellite I are plotted in Fig. 3. Some thermal control surfaces degrade at a higher rate initially and with time, a roll off is seen in the absorptance-versus-time curve. An exponential roll off fit of the form

$$a_s = a_o + (a_m - a_o)(1 - e^{-t/\tau}) \qquad (1)$$

is used to fit the date. Table 2 lists the coefficients of this expression, the emissivity of each thermal control surface sample, the laboratory measured a_s and maximum equivalent sun-hours.

The increase in a_s for the two PDPS-coated samples on Satellite I is due to degradation caused by the PDPS, as well as

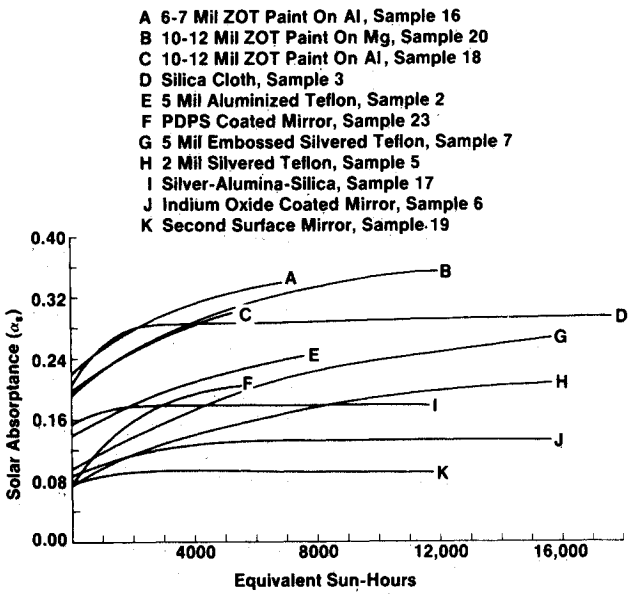

Fig. 2 Updated calorimeter data of representative flight samples.

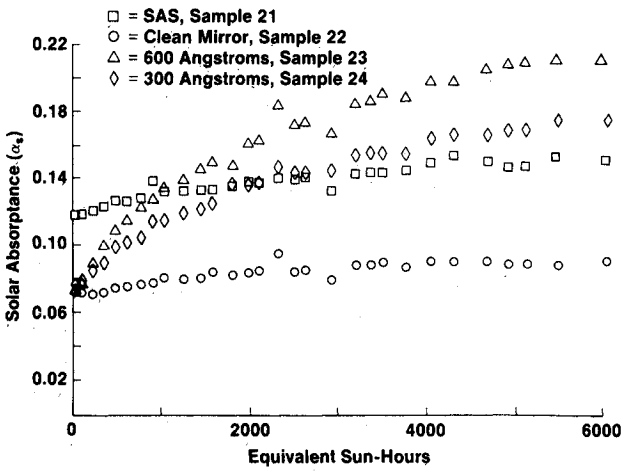

Fig. 3 Satellite I calorimeter samples.

degradation caused by all other factors. The following equation is used to determine the degradation caused by the PDPS coating:

$$\Delta a_s = a_{\text{actual}} - a_o - \Delta a_{\text{clean mirror}} \qquad (2)$$

where $\Delta a_{\text{clean mirror}}$ is the contamination from all other factors. Figure 4 shows the degradation due to the PDPS coating. For this silicon based polymer, an approximate 0.02 increase in a_s occurs for every 100 Å of PDPS after 6000 equivalent sun-hours of exposure.

Thermal Control Surface Samples Discussion

Second-Surface Mirror Samples

Since extensive a_s data are available for space-stable second-surface mirrors, second-surface mirrors are selected as the baseline sources of calorimetric data for inter-satellite reference and comparison. Figure 5 compares the a_s-versus-equivalent-sun-hour curves for several second-surface mirror samples. The second-surface mirror sample for Satellite I (sample 22) shows performance similar to that of the other second-surface mirror samples. The initial rise in a_s for the NAVSTAR fused silica mirror is greater than that of the other mirror samples.[7] The NAVSTAR orbit is different than the orbits of the other satellites, with a correspondingly different

Table 1 Calorimeter sample description

Sample no.	Thermal control surface sample	Satellite	Method of application
1	0.002-in. silvered Teflon	D	Nickel-powder-filled acrylic adhesive
2	0.005-in. aluminized Teflon	D	Nickel-powder-filled acrylic adhesive
3	Silica cloth (GE Astroquartz 581)	D	Heat-laminated on 0.001 in. aluminized Teflon
4	Silica cloth (GE Astroquartz 581)	D	Double-faced tape with SR 585 adhesive
5	0.002-in. silvered Teflon	E	Nickel-powder-filled acrylic adhesive
6	Indium-tin oxide front-coated mirror	E	RTV-566 adhesive
7	0.005-in. embossed silvered Teflon	E	Pressure-sensitive P/223 tape
8	Second-surface mirror	E	RTV-566 adhesive
9	ZOT paint (8-10 mil thick)[a]	F	On 6061-T6 aluminum
10	ZOT paint (8-10 mil thick)[a]	F	On 6061-T6 aluminum
11	Second-surface mirror	F	RTV-566 adhesive
12	ZOT paint (8-10 mil thick)[a]	F	On AZ31B magnesium
13	Second-surface mirror	G	RTV-566 adhesive
14	ZOT paint (10-12 mil thick)[a]	G	On 6061-T6 aluminum
15	Second-surface mirror	G	RTV-566 adhesive
16	ZOT paint (6-7 mil thick)[a]	G	On 6061-T6 aluminum
17	Silver-alumina-silica	H	Vapor-deposited on anodized 6061 aluminum
18	ZOT paint (10-12 mil thick)[a]	H	On 6061-T6 aluminum
19	Second-surface mirror	H	RTV-566 adhesive
20	ZOT paint (10-12 mil thick)[a]	H	On AZ31B magnesium
21	Silver-alumina-silica	I	Vapor-deposited on reflector grade 1100 aluminum
22	Second-surface mirror	I	RTV-566 adhesive
23	Second-surface mirror with 600 Å PDPS	I	Adhesion promoter[b]
24	Second-surface mirror with 300 Å PDPS	I	Adehsion promoter[b]

[a]Zinc orthotitanate pigment in potassium silicate binder YB-71 manufactured by Illinois Institute of Technology Research.
[b]10% hexamethyl disilizane in xytene.

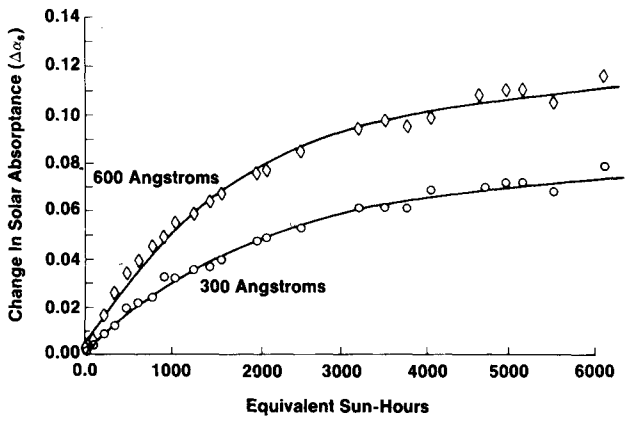

Fig. 4 Degradation due to polydimethylphenyl siloxane.

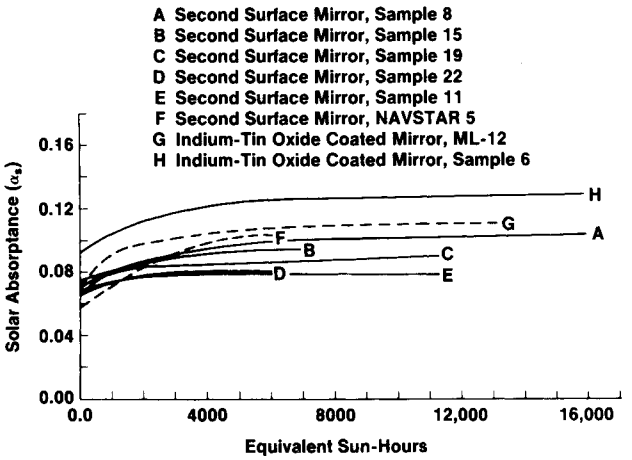

Fig. 5 Comparison of mirror samples.

contamination profile. The indium-tin oxide front-coated mirror samples (G and H) degraded at a different rate than surfaces which did not have this conductive coating.

Metalized Teflon

Figure 6 shows the a_s values for aluminized and silvered Teflon samples as a function of equivalent sun-hours. The samples have similar a_s rise rates, but different initial a_s values. Silvered Teflon performs better than aluminized Teflon, and the 2-mil silvered Teflon performs better than the embossed 5-mil silvered Teflon. The embossed surface was developed to provide a flexible surface over a large temperature cycle, but this embossed surface significantly decreases performance. The ML-12 and NAVSTAR samples show similar initial a_s in which the same trends are apparent.[6,7] The indium-tin oxide front-coated silvered Teflon shows a higher initial a_s value but its a_s rise rate is similar to that of the other samples and consistent with the performance of the indium oxide front-coated mirror shown in Fig. 5.

Table 2 Solar absorptance (a_s) and emissivity (ϵ) data. $a_s = a_o + (a_m - a_o)\,(1^{-e-t/\tau})$

Sample no.	Thermal control surface sample	a_o	a_m	τ	ϵ	$\Sigma\kappa\chi$. a_s	Max. ESH
1	0.002-in. silvered Teflon	0.080	0.241	12,123	0.66	0.068	9,300
2	0.005-in. aluminized Teflon	0.163	0.316	9,525	0.80	0.144	15,500
3	Silica cloth (GE Astroquartz 581)	0.200	0.276	855	0.86	0.197	17,750
4	Silica cloth (GE Astroquartz 581)	0.180	0.268	828	0.86	0.165	17,750
5	0.002-in. ailvered Teflon	0.085	0.246	8,769	0.66	0.066	15,500
6	Indium-tin oxide front-coated mirror	0.096	0.133	2,265	0.79	0.082	18,000
7	0.005-in. embossed silvered coated mirror	0.108	0.297	7,467	0.80	0.095	15,500
8	Second-surface mirror	0.077	0.103	3,138	0.79	0.068	18,000
9	ZOT paint (8-10 mil thick)	0.202	0.336	5,108	0.91	0.194	5,800
10	ZOT paint (8-10 mil thick)	0.189	0.351	4,885	0.91	0.181	5,800
11	Second-surface mirror	0.067	0.077	2,485	0.79	0.068	5,800
12	ZOT paint (8-10 mil thick)	0.193	0.373	4,926	0.91	0.188	11,000
13	Second-surface mirror	0.069	0.090	1,228	0.79	0.068	6,600
14	ZOT paint (10-12 mil thick)	0.180	0.311	3,562	0.91	0.167	7,000
15	Second-surface mirror	0.070	0.090	905	0.79	0.068	6,600
16	ZOT paint (6-7 mil thick)	0.222	0.372	4,106	0.91	0.214	7,000
17	Silver-aluminapsilica	0.150	0.178	669	0.79	0.158	11,800
18	ZOT paint (10-12 mil thick)	0.183	0.270	1,269	0.91	0.167	5,200
19	Second-surface mirror	0.072	0.089	1,344	0.79	0.068	11,200
20	ZOT paint (10-12 mil thick)	0.202	0.385	7,053	0.91	0.167	12,000
21	Silver-alumina-silica	0.119	0.154	2,724	0.79	0.116	6,000
22	Second-surface mirror	0.069	0.091	1,729	0.79	0.056	6,000
23	Second-surface mirror with 600 Å PDPS	0.075	0.217	2,088	0.79	0.055	6,000
24	Second-surface mirror with 300 Å PDPS	0.075	0.177	2,169	0.79	0.056	6,000

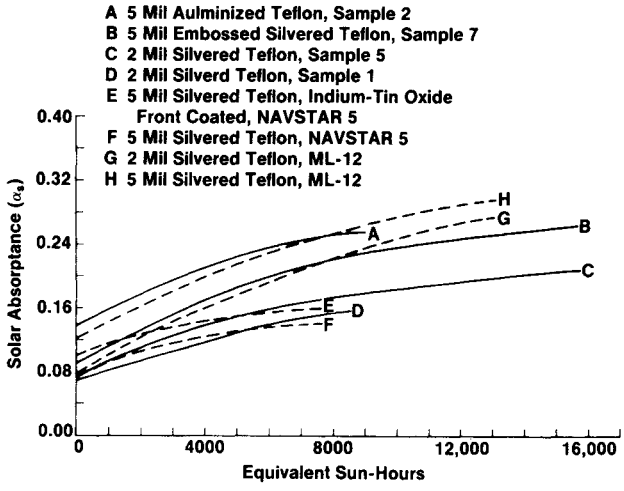

Fig. 6 Comparison of silvered and aluminized Teflon.

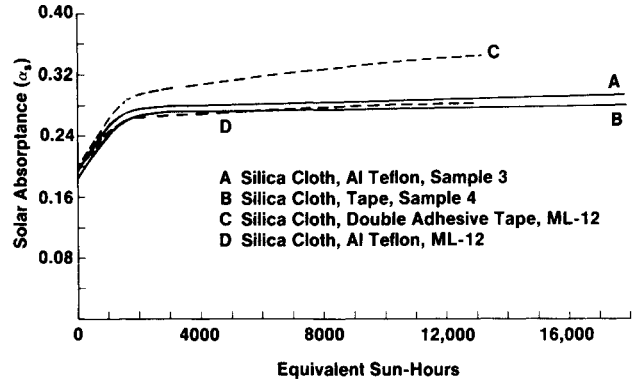

Fig. 7 Comparison of silica cloths.

Silica Cloth

Shown in Fig. 7 are a_s values as a function of equivalent sun-hours for the silica cloth samples. The two calorimeter silica cloth samples exhibit similar behavior. The ML-12 silica cloth with tape had similar initial a_s but degraded at a higher rate than the calorimeter silica cloth samples.[6] The addition of the aluminized Teflon to the ML-12 silica cloth greatly enhanced performance, as compared to the performance of the ML-12 silica cloth with tape.

Zinc Orthotitanate Paint

The ZOT samples are presented in Fig. 8. Samples with less than an 8-mil thickness of ZOT have a higher initial a_s, but the degradation rate does not seem to be a function of ZOT thickness. Although ZOT on an aluminium substrate has the same initial properties as on a magnesium substrate, the a_s of the magnesium samples degrades at a higher rate. The substrate material appears to play an important role in the a_s of the ZOT thermal control surface. A comparison is also made with

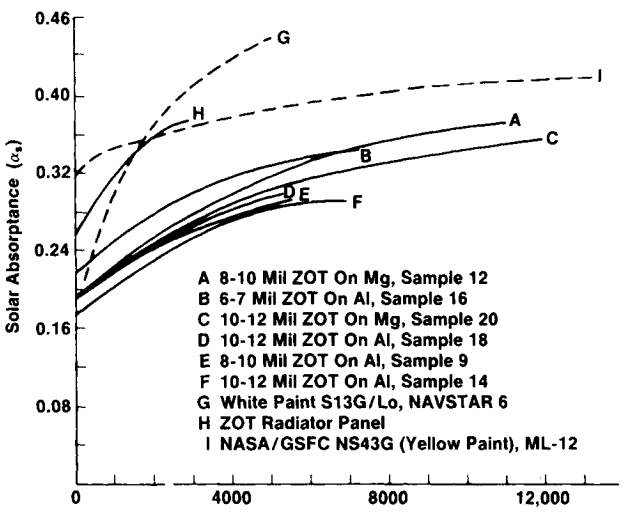

Fig. 8 Comparison of white paints.

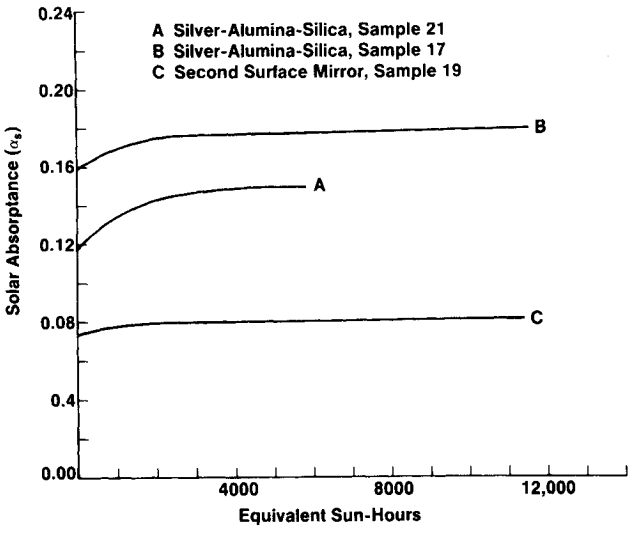

Fig. 9 Comparison of silver-alumina-silica samples.

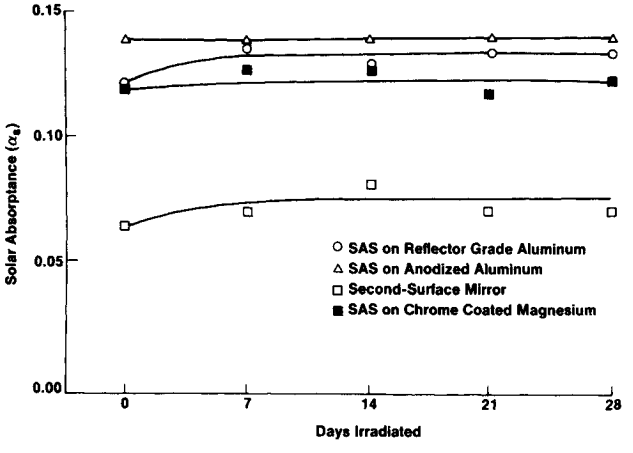

Fig. 10 Solar absorptance measurements for laboratory irradiation of SAS.

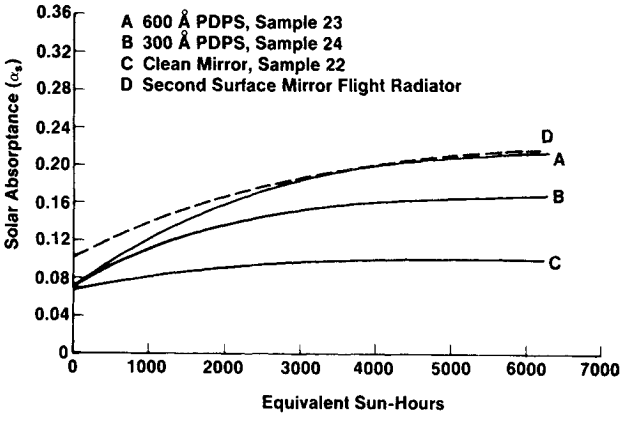

Fig. 11 Comparison of PDPS samples.

a ZOT-coated panel on a similar satellite. The ZOT panel is located closer to the electronics enclosure than the calorimeter, making it more susceptible to outgassing from this area. Also shown are data for S13G/LO on NAVSTAR[6] and a yellow paint on ML-12.[6]

Silver-alumina-silica

A comparison of the a_s as a function of equivalent sun-hours of two SAS samples is plotted in Fig. 9. These two samples show similar degradation rise rate behavior, but different values of initial a_s. The SAS on reflector grade 1100 aluminum (sample 21), has a lower initial a_s than the SAS on anodized 6061 aluminum (sample 17). The substrate finish and coating quality determines the initial a_s for similar thermal control surface coatings. Laboratory SAS samples show that the SAS on the reflector grade 1100 aluminium base material produces lower initial a_s than SAS on the anodized aluminum, as also seen on orbit.[8] Laboratory irradiation of SAS samples of different substrates shows similar degradation rates (see Fig. 10). The SAS a_s degrades at a very slow rate, just slightly higher than the rate of a clean mirror.

Precontaminated Mirror

Figure 11 shows the PDPS-coated second-surface mirror samples compared to a mirrored surface on the cylindrical flight radiator that houses the calorimeter on Satellite I. This mirrored radiator surface exhibits degradation rates higher than that of the clean mirror sample and the degradation rates are similar to the PDPS samples. The calorimeter location is less susceptible to contamination than other radiator zones, particularly the one shown in Fig. 11 (Curve D).[11] The radiator data and the PDPS samples data correlate well after about 2000 sun-hours. Early data, however, show a sharp rise in the a_s of the PDPS-coated samples, whose a_s started at approximately the same initial a_s as that of the clean mirror sample. The first measurement of a_s on the radiator was taken at two months after launch and is significantly higher than the a_s on a clean mirror sample.

Since the initial a_s values of the calorimeter samples and the radiator surface are different, a contaminant(s) other than PDPS may have been deposited on the radiator. The radiator surface could have been damaged or contaminated shortly before or during launch, resulting in a higher initial a_s. Laboratory irradiation of second-surface mirror samples contaminated with propellant volatile condensible material (VCM) deposits demonstrated a degradation curve similar to that of the degraded radiator surface on Satellite I[9] (see Fig. 12). Unlike the PDPS-contaminated samples, the initial a_s on the VCM-contaminated samples is higher than the a_s on the clean mirror sample and is consistent with radiator surface data. This would support the assumption that the materials deposited on the calorimeter on Satellite I are other than PDPS.

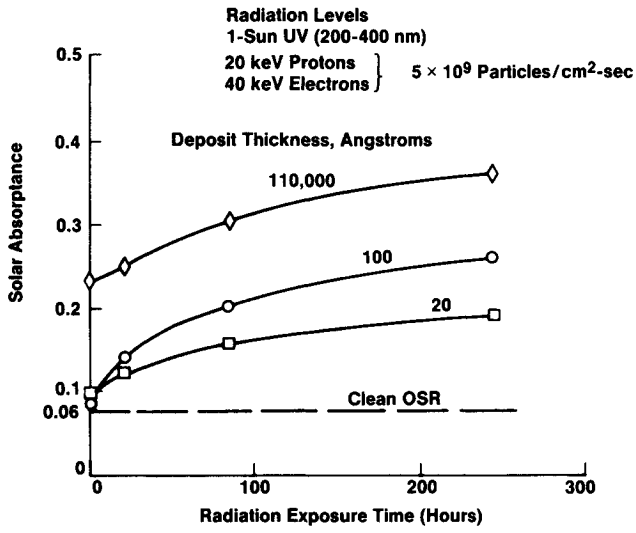

Fig. 12 Second-surface mirror samples contaminated with propellant VCM deposits

Design Application and Results Verification

Passive radiators are commonly used for temperature control on satellites and spacecraft. The heat generated by the satellite and the heat absorbed from the sun, albedo, earthshine must be rejected. Control of this heat rejection is accomplished by choosing the appropriate thermal control surface for the radiator. Usually a low a_s is desired to minimize the influence of the solar heat flux on radiator performance. A high emissivity value is usually required to keep the size and weight of the radiator at a minimum. The next consideration is the performance of the thermal control surface, over time in the space environment. In order to design a radiator to meet operational life requirements, which means maintaining given temperature ranges, a good knowledge of thermal control surface degradation rates is necessary. A consistent set of long-life data on a number of thermal control surfaces has been presented in this paper.

The a_s degradation equations that were developed from the calorimeter data analysis are currently used to accurately and repeatedly predict the thermal behavior of satellite and spacecraft thermal control surfaces. In the following example, the ZOT on aluminum (8-10 mils) a_s degradation equation and the second-surface mirror a_s degradation equation, from the calorimeter data analysis, are used in the thermal math model of another satellite of the same series. Figure 13 shows the excellent correlation between the diurnal temperatures for a radiator coated with ZOT, predicted by the model, and actual flight data for both 361 equivalent sun-hours and 2130 equivalent sun-hours. The data also match very well (see Fig. 14) for a second-surface mirror radiator surface on a cylindrical portion of the satellite.

It is obvious from the data presented above that the calorimeter data collected on these flights are design tools of major significance. In early design stages, these data can be used to choose appropriate thermal control surfaces and to make subsequent predictions of the long-life performance of satellite and spacecraft thermal control surfaces. However, thermal control surfaces that are contaminated will have higher degradation rates. A correction factor must be applied, then, in cases where contamination is expected. The data presented in this report on contaminated thermal control surfaces is the first step to quantify this correction factor. Further studies in this area are needed.

Conclusion

The calorimeter data presented provide both qualitative and quantitative insight into the behavior of thermal control surfaces in the space environment. An efficient calorimeter that thermally isolates clean thermal control surface samples from the satellite can enhance the likelihood of the development of accurate and reliable thermal control surface performance data. The relative performance of the evaluated thermal control surfaces and insight into degradation and contamination mechanisms of such surfaces may be discerned from these results. The solar absorptivity degradation equations determined from these data have been used successfully to predict satellite orbital temperatures. Consequently, these results provide a data base that can be used to design reliable, long-life thermal control systems for satellites.

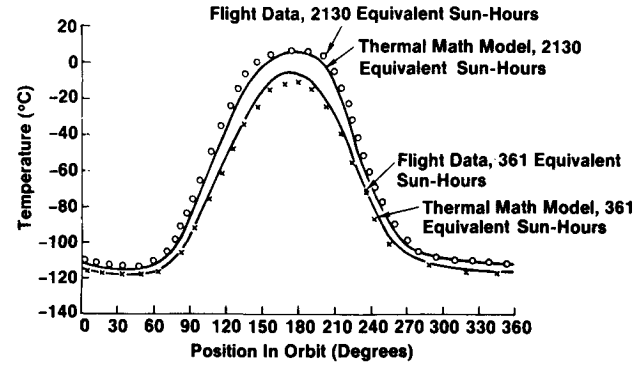

Fig. 13 ZOT on aluminum a_s equations applied.

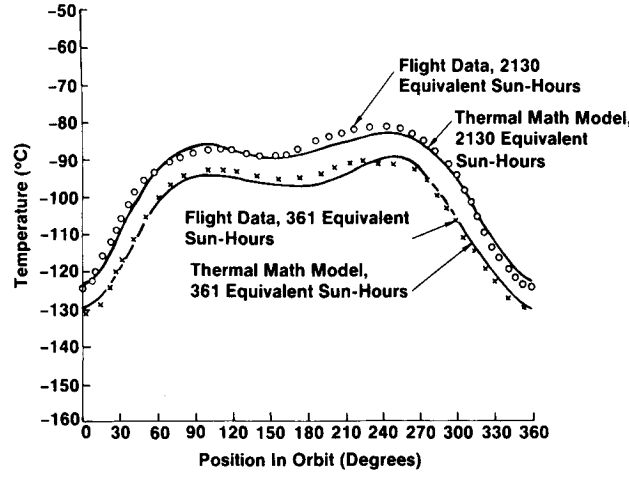

Fig. 14 Second-surface mirror a_s equations applied.

Acknowledgment

This work was performed by Aerojet ElectroSystems Space Surveillance Division, Azusa, California, under Contract F04701-84-C-0034 from the United States Air Force Space Division.

References

[1]Ahern, J.E. and Karperos K., "Calorimetric Measurements of Thermal Control Surfaces on Operational Satellites," *Progress in Astronautics and Aeronautics*, Vol. 91, edited by J.A. Roux and T.D. McCay, AIAA, Washington, DC, 1984, pp. 235-260.

[2]Curran, D.G.T. and Millard, J.M., "Results of Contamination/Degradation Measurements on Thermal Control Surfaces of an Operational Satellite," 12th Thermophysics Conference, Albuquerque, New Mexico, AIAA Paper No. 77-740, June 1977.

[3]Haas, G., Heaney, J.B., and Triolo, J.J., "Evaporated A_g Coated with Double Layers of Al_2O_3 and Silicon Oxide to Produce Surface Films with low Solar Absorptivity and High Emissivity," *Optics Communications,* Vol. 8, July 1987, p. 183.

[4]Haas, G., Ramsey, J.B., Heaney, J.B., and Triolo, J.J., "Reflectance, Solar Absorptivity and Thermal Emissivity of S_1O_2-Coated Aluminum," *Applied Optics,* Vol. 8, Feb. 1969, p. 275.

[5]Haas, G., Ramsey, J.B., Heaney, J.B., and Triolo, J.J., "Thermal Emissivity and Solar Absorptivity of Aluminum Coated with Double Layer of Aluminum Oxide and Silicon Oxide," *Applied Optics,* Vol. 10, June 1971, p. 1296.

[6]Hall, D.F. and Fote, A.A., "Long-Term Performance of Thermal Control Coatings at Geosynchronous Altitude," 4th Joint Thermophysics and Heat Transfer Conference, Boston, MA, AIAA Paper No. 86-1356, June 1986.

[7]Pence, W.R. and Grant, T.J., "α Measurements of Thermal Control Coatings on NAVSTAR Global Positioning System Spacecraft," 16th Thermophysics Conference, Palo Alto, CA, AIAA Paper No. 81-69, June 1981.

[8]Barsh, M.K. and Mossman, D.L., "Geosynchronous Orbit and Laboratory Irradiation of SAS Quarter-Wave Thermal Control Surfaces," 20th Thermophysics Conference, Williamsburg, VA, AIAA Paper No. 85-950, June 1986.

[9]Neff, J., Mullen, C. and Fogdall, L., "Effects of a Simulated Synchronous Altitude Environment on Contaminated Optical Solar Reflectors," AIAA Paper 85-0954, June 1985.

[10]Mossman, D.L., Bostic,. H.D., and Carlos, J.R., "Contamination Induced Degradation of Optical Solar Reflectors in Geosynchronous Orbit," SPIE Conference 777, Orlando, FL, May 1987.

[11]Ahern, J.E., Belcher, R.L. and Ruff, R.D., "Analysis of Contamination Degradation of Thermal Control Surfaces on Operational Satellites," *Spacecraft Contamination: Sources and Prevention, Progress in Astronautics and Aeronautics,* Vol. 91, edited by J.A. Roux and T.D. McCay, AIAA, Washington, DC, 1984, pp. 96-107.

TO APPEAR IN FORTHCOMING ISSUES OF THIS JOURNAL

Two-Wavelength Holographic Measurement of Temperature and Concentration During Alloy Solidification by A. Ecker.

Correlation of the Gap Conductance Integral for Conforming Rough Surfaces (TN) by K. J. Negus and M. M. Yovanovich.

Perturbation Analysis of Tapered Fins with Nonlinear Thermal Properties (TN) by K. D. Hagen.

Analyses of Two-Dimensional Steady-State Heat Transfer in a Rectangular Region with Convective Boundary Conditions by C. L. Ko and C. W. Bert.

Approximate Method for Transient Conduction in Arbitrarily Shaped Solids with a Volumetric Heat Source (TN) by K. Taghavi and R. A. Altenkirch.

Unsteady Heat Transfer Coefficient Estimation for Long Duration by J. K. Hodge, A. J. Chen, and J. R. Hayes.

Unsteady Heat Transfer Problems Related to a High Power Laser Flow Loop by S. S. Munukutla and R. Venkataraman.

Numerical Models of Two Complex Hypersonic Flow Fields by M. G. Macaraeg.

Ablation with a Large Fraction of Solid Removal by G. Y. Jumper and J. E. Hitchcock.

Cavitation of Liquid Streams in a Vacuum (TN) by M. Dixon, H. Legge, G. Koppenwallner, and E. P. Muntz.

Transient Condensation of a Laminar Film on a Vertical Plate by J. G. Reed and R. M. Gerner.

Steady Conjugate Heat Transfer in Fully Developed Laminar Pipe Flows (TN) by J. C. Kuo and T. F. Lin.

Analysis of Turbulent Pipe Flow with a Variable Heat Transfer Coefficient Using Integral Equations by J. Beale and B. Vick.

Natural Convection of a Variable Property Gas in Asymmetrically Heated Square Cavities (TN) by B. Farouk and T. Fusegi.

Three-Dimensional Natural Convection Experiments in an Enclosure by D. Sadowski, D. Poulikakos, and M. Kazmierczak.

Study of Heat Transfer from a Finned Rotating Cylinder by J. V. Murthy.

A 3500K High Frequency Induction Heated Blackbody Source (TN) by G. Shijie, F. Guoyi, and Z. Qiren

Radiation View Factors from Differential Plane Sources to Disks—A General Formulation (TN) by M. H. N. Naraghi.

Simple Model for the Exchange of Radiant Energy Between Particles (TN) by D. L. Cohen.

Radiation Heat-Transfer Model for Fibers Oriented Parallel to Diffuse Boundaries by S. C. Lee.

Source Expansion Solutions for Radiative Transfer in Slab, Spherical, and Cylindrical Geometries (TN) by A. Kisomi and W. H. Sutton.

Substrate Effects on Two-Dimensional Radiative Backscattering by H. F. Nelson and D. C. Look.